



Published in final edited form as:

Invest Ophthalmol Vis Sci. 2009 April ; 50(4): 1531–1539. doi:10.1167/iovs.08-2173.

Localization of a Gene for Keratoconus to a 5.6-Mb Interval on 13q32

Marzena Gajecka^{1,2}, Uppala Radhakrishna³, Daniel Winters¹, Swapan K. Nath⁴, Malgorzata Rydzanicz¹, Uppala Ratnamala³, Kimberly Ewing⁴, Andrea Molinari⁵, Jose A. Pitarque⁵, Kwanghyuk Lee⁶, Suzanne M. Leal⁶, and Bassem A. Bejjani^{1,7}

¹Basic Medical Sciences Program, WWAMI (Washington, Wyoming, Alaska, Montana, and Idaho), Washington State University, Spokane, Washington ²Institute of Human Genetics, Polish Academy of Sciences, Poznan, Poland ³Cancer Center, Creighton University, Omaha, Nebraska ⁴Arthritis and Immunology Research Program, Oklahoma Medical Research Foundation, Oklahoma City, Oklahoma ⁵Department of Ophthalmology, Hospital Metropolitano, Quito, Ecuador ⁶Department of Molecular and Human Genetics, Baylor College of Medicine, Houston, Texas ⁷Sacred Heart Medical Center, Spokane, Washington

Abstract

Purpose—Keratoconus (KTCN) is a noninflammatory thinning and anterior protrusion of the cornea that results in steepening and distortion of the cornea, altered refractive powers, and reduced visual acuity. Several loci responsible for a familial form of KTCN have been mapped, however; no mutations in any genes have been identified for any of these loci. There is also evidence that *VSX1* and *SOD1* may be involved in the etiology of KTCN. The purpose of this study was to verify the available data and to identify a new keratoconus susceptibility locus.

Methods—KTCN without other ocular or systemic features was diagnosed in 18 families. *VSX1* and *SOD1* sequencing was performed on affected individuals and control subjects. Genomewide linkage analysis was then performed in all families using polymorphic microsatellite markers with an average spacing of 5 cM. Next, single-nucleotide polymorphism (SNP) arrays, fluorescence in situ hybridization (FISH) analysis, and a comparative genomic hybridization array were used in one family to assess a candidate region on 13q32.

Results—All previously reported KTCN loci were excluded. *VSX1* and *SOD1* were sequenced, and no potentially functional variants were found. One KTCN family yielded a maximum multipoint parametric LOD score of 4.1 and multipoint non-parametric linkage (NPL) LOD score of 3.2. Multipoint linkage and haplotype analysis narrowed the locus to a 5.6-Mb region between the SNPs rs9516572 and rs3825523 on 13q32.

Conclusions—The results exclude *VSX1* and *SOD1* as potential disease-causing genes in these families and localize a novel gene for keratoconus to a 5.6-Mb interval on 13q32.

Corresponding author: Bassem A. Bejjani, Washington State University Spokane, Box 1495, Spokane, WA 99210-1495; bejjani@wsu.edu.

Disclosure: M. Gajecka, None; U. Radhakrishna, None; D. Winters, None; S.K. Nath, None; M. Rydzanicz, None; U. Ratnamala, None; K. Ewing, None; A. Molinari, None; J.A. Pitarque, None; K. Lee, None; S.M. Leal, None; B.A. Bejjani, None

Keratoconus (KTCN) is a noninflammatory thinning and consequent bulging of the cornea that results in distortion of the corneal surface, altered refractive powers of the eye (both axial and refractive), and reduced visual acuity. In more advanced cases, corneal scarring further reduces visual acuity. Symptoms are highly variable and depend on the stage of progression of the disorder.^{1,2} The trait has an incidence of approximately 1 in 2000 individuals and is the most common indication for corneal transplantation in the United States.¹ Both, genetic and environmental factors are associated with KTCN. More than two dozen syndromes are associated with KTCN, including Down syndrome,³ Leber's congenital amaurosis,⁴ connective tissue disorders including osteogenesis imperfecta,⁵ Gapo syndrome,⁶ and some subtypes of Ehlers-Danlos syndrome.^{7,8} However, in most patients KTCN is an isolated ocular disorder and not a feature of a specific syndrome. Clinical studies have suggested that KTCN is associated with contact lens wear, chronic eye rubbing, and atopy of the eye.^{1,9,10} Despite extensive study, the pathophysiological processes and the genetic etiology underlying KTCN have yet to be elucidated. Ninety percent of pedigrees with familial KTCN display an autosomal dominant inheritance with reduced penetrance.^{11,12}

Six loci responsible for a familial form of KTCN have been mapped to 16q22.3-q23.1 (KTCN2; MIM [Mendelian Inheritance in Man] 608932), 3p14-q13 (KTCN3; MIM 608586), 2p24 (KTCN4; MIM 609271), 5q14.3-q21.1, 15q23-24, and 20q12.11,¹³⁻¹⁸ However, to date, no mutations in any genes have been identified for any of these loci. There is also evidence that *VSX1* on 20p11.2 (KTCN1; MIM 605,020) and *SOD1* (MIM 147,450) on 21q22.11 are involved in the etiology of KTCN.^{18,19}

We analyzed 18 Ecuadorian families with nonsyndromic KTCN. These families displayed an autosomal dominant inheritance pattern with reduced penetrance. No potentially functional variants were found in *VSX1* and *SOD1*. Genome-wide linkage analysis provided significant evidence for a novel locus on 13q32 which maps to a 5.6-Mb genomic region.

Methods

Clinical Evaluation of KTCN Families

Eighteen families from Ecuador with KTCN were ascertained and examined in the Hospital Metropolitano (Quito, Ecuador). All provided informed consent after the possible consequences of the study were explained, in accordance with the Declaration of Helsinki. All study subjects underwent a complete ophthalmic evaluation that included visual acuity (VA), IOP, biomicroscopic evaluation, and fundus examination with dilation. In addition, affected individuals and individuals with a suspected corneal abnormality underwent a topographic study (Humphrey Atlas Topograph; Carl Zeiss Meditec, Jena, Germany) with a computer-assisted videokeratoscope. Individuals with KTCN showed conical protrusion of the cornea, prominent corneal nerves, and corneal thinning with or without stromal scar tissue. The diagnosis of KTCN was established in subjects with at least two of the following topographic characteristics: (1) the curvature of the cornea more than 47 D (normal, ~43 D), (2) acentric or irregular corneal video keratography (CVK) shapes, and (3) inferior-superior (IS) value differences of 3 D, 3 mm below and above the center. We also examined all first-

degree relatives (parents, siblings, and grandparents) of affected individuals over the age of 11.

Pedigrees are shown in Figures 1 and 2. Since the age of onset of KTCN is at puberty,² children younger than 16 years and unaffected were scored as “unknown phenotype status.” Deceased individuals and individuals who did not wish to participate in the study were considered to have unknown affection status for the purpose of linkage analysis. Blood samples were collected from all participating family members after informed consent for the genetic studies was given.

Sequencing Analyses and Genome Wide Screen with Fluorescent Microsatellite Markers

Genomic DNA was prepared with a DNA extraction kit (Puregene; Qiagen, Inc., Valencia, CA). A total of 143 samples from 18 families were included in the analysis; 76 affected individuals, and 67 unaffected individuals. The coding regions and all splice junctions of *VSX1* were sequenced before mapping studies in 57 affected individuals from all 18 families, in three unaffected individuals and in 20 unrelated Ecuadorian control subjects with no ocular abnormalities. *SOD1* was also sequenced in two individuals with KTCN from each family (36 individuals). All exons of *VSX1* and *SOD1* as well as the intron-exon junctions were sequenced as described elsewhere.¹⁹ PCR-based sequencing was performed with dye terminator chemistry (Big Dye Terminator Kit; Applied Biosystems, Inc. [ABI], Foster City, CA) and visualized on a genetic analyzer (Prism 3100; ABI). The results were analyzed on computer (Sequencher software; Gene Codes Corp., Ann Arbor, MI).

Before the genomewide scan, targeted genotyping was performed with 120 polymorphic microsatellite markers that map to published candidate loci for familial KTCN on 16q22.3-q23.1, 3p14-q13, 2p24, 5q14.3-q21.1, 15q23-24, 20q12, 20p11.2 (*VSX1*), and 21q22 (*SOD1*). These 120 microsatellite markers consisted of 48 microsatellite markers (Prism Linkage Mapping Set, ver. 2.5; ABI) and 72 additional markers (Rutgers Combined Linkage-Physical Map, Build 36; <http://compgen.rutgers.edu/maps/> provided in the public domain by the department of Genetics, Rutgers University, Piscataway, NJ),²⁰ allowing for an average spacing of 1 to 1.5 cM across the published candidate loci for familial KTCN. Custom-designed fluorescence-labeled primers were obtained from Integrated DNA Technologies (Coralville, IA).

A genomewide screen was performed by genotyping the KTCN families with the remaining 763 fluorescently labeled PCR primer pairs (Prism Linkage Mapping Set, ver. 2.5; ABI) which are spaced approximately at 5 cM across the human genome. In both the targeted genotyping and genomewide screen, amplified products were visualized on a genetic analyzer (Prism 3100; ABI, equipped with 16 capillaries, a 36-cm array, POP-4 polymer, and GeneScan 400 HD [Rox] Size Standard). DNA amplifications of microsatellite markers were performed according to standard procedures in a total volume of 11 μ L with one of two PCR reagents (either True Allele PCR Premix or Master Mix AmpliTaq Gold reagent; ABI). The fragments were then sized on computer (PRISM GeneScan and Genotyper Software; ABI).

To reduce the candidate genomic region on 13q32, we selected polymorphic markers from the Rutgers Combined Linkage-Physical Map (Build 36)20 to achieve a spacing of one microsatellite marker every 0.5 to 1.0 cM. Seventeen of these markers were informative and are shown in Table 1.

Genome-wide Genotyping in Family KTCN-014

To further narrow the region of interest, a single-nucleotide-polymorphism (SNP) array (Affymetrix, GeneChip Mapping 250K Nsp Array) containing 262,000 SNPs was used to genotype 10 affected and 11 unaffected individuals from KTCN-014 (Fig. 2).

These SNP markers are equally distributed in the genome with a median physical distance between SNPs of 4.8 kb, an average distance between SNPs of 11.2 kb, and an average heterozygosity of 0.30 (Affymetrix, Santa Clara, CA). The assay was performed with 250 ng of genomic DNA, and more than 99% of the SNPs were determined unequivocally for each sample. Scanned images were processed with gene microarray software (Affymetrix). The data were then analyzed on computer (GDAS ver. 2 software; GeneChip Data Analysis; Affymetrix).

Cytogenetic Analysis and Array Comparative Genomic Hybridization

To evaluate the possibility of copy number variation in the examined chromosome region fluorescence in situ hybridizations (FISH) was performed. Three affected (KTCN 14-06, 14-16, and 14-18) and two unaffected (KTCN 14-02, 14-20) individuals were tested with eight fosmid (G248P82021F1, G248P8010G10, G248P87136A3, G248P8410H5, G248P86109F5, G248P88996E4, G248P86068C11, and G248P8720B7) and two BAC clones (RP11-123H22 [AL162717] and RP11-49K6 [AQ051918]) corresponding to 13q31-13q33. The probe assignment in the Human Mar 2006 (hg18; UCSC Genome Browser Web site, <http://genome.ucsc.edu/>) assembly was confirmed by metaphase FISH, and then with interphase FISH with the probe combination performed as described elsewhere.²¹ Two hundred interphase cells per slide were counted.

Array comparative genomic hybridization (array CGH) was performed to assess the copy number differences at chromosome 13 in three affected (KTCN 14-03, 14-05, and 14-07) and two unaffected (KTCN 14-01, 14-14) individuals. Fine-tiling array CGH for chromosome 13 (human chromosome 13 CGH project) with ultra-high-density and long oligo probes (interval spacing: 221 bp [mean]; 225 bp [median]) was performed at NimbleGen Systems, Inc. (Reykjavik, Iceland).

Linkage Analysis

PEDCHECK²² was used to identify Mendelian inconsistencies, and the MERLIN²³ program was used to detect double recombination events over short genetic distances that were probably due to genotyping errors. For the parametric linkage analysis an autosomal dominant mode of inheritance with reduced penetrance (0.8) and phenocopies (0.01) and a disease allele frequency of 0.0001 were used. In addition, for the parametric linkage analysis an affected only analysis was performed under an autosomal dominant mode of inheritance allowing for phenocopies. For the microsatellite marker, two-point parametric linkage

analysis under homogeneity was performed with the MLINK program of the FASTLINK computer package,²⁴ and parametric linkage analysis allowing for linkage admixture was performed using HOMOG.²⁵ For microsatellite and SNP marker loci, multipoint non-parametric and parametric affected only linkage analysis under linkage homogeneity, and admixture was performed with ALLEGRO.²⁶ SIMWALK2^{20,27} was used to perform parametric analysis with reduced penetrance, because of the large size of the pedigree. ALLEGRO²⁶ uses the Lander-Green algorithm, which limits the size of pedigree that can be analyzed in small- to medium-sized pedigrees. The microsatellite marker allele frequencies were estimated from the founders and reconstructed genotypes of founders from the 18 Ecuadorian pedigrees. Because the SNP markers were genotyped only in family 14, equal allele frequencies were used in the analysis. For both the microsatellite and SNP marker loci genetic map distances were then derived from the Rutgers combined linkage-physical map of the human genome,²⁰ either directly or by interpolation. Haplotypes were reconstructed using the SIMWALK2 program.^{27,28}

Web Resources

The URLs for data presented herein are as follows: Affymetrix, Santa Clara CA, <http://www.affymetrix.com/products/arrays/specific/250k.affx/>; Ensemble,²⁹ <http://www.ensembl.org/>; Genome Database (<http://www.gdb.org/>); MERLIN, <http://www.sph.umich.edu/csg/abecasis/Merlin/>; National Center for Biotechnology Information, Bethesda, MD, Build 36, <http://www.ncbi.nih.gov/>; and Online Mendelian Inheritance in Man (OMIM), <http://www.ncbi.nlm.nih.gov/OMIM/>.

Results

Initial Candidate Gene Mutation Analyses

Before the genome-wide scan, the two known candidate genes *VSX1* and *SOD1* were excluded as causing KTCN in these families. Novel polymorphism 174G>T (NM_014588), and p.P58P was identified in one affected individual and one control subject. There were three previously reported polymorphisms. Polymorphism c.18 G>T (NM_014588), and p.S6S (rs8123716) was identified in five affected individuals and four control subjects. Polymorphism c.546A>G (NM_014588), and p.F182F (rs12480307) was identified in 26 affected individuals and 8 control subjects. Polymorphism c.627+23G>A (NM_014588), rs6138482, was identified in 19 affected individuals and 9 control subjects. No variants in *SOD1* were found.

Targeted Genotyping and Genome-Wide Screening

Targeted genotyping with polymorphic markers corresponding to published candidate genomic regions for familial KTCN on 20p11.2 (KTCN1, *VSX1*), 16q22.3-q23.1 (KTCN2), 3p14-q13 (KTCN3), 2p24 (KTCN4), 5q14.3-q21.1, 15q23-24, 20q12, and 21q22 (*SOD1*) revealed no evidence of linkage (LOD < 0.5) and did not produce parametric LOD scores > 0.5 between KTCN and these loci (data not shown).

The analysis of 17 of 18 KTCN families did not reveal evidence of linkage (LOD scores < 0.5), both for parametric and nonparametric linkage analysis under linkage homogeneity and allowing for linkage admixture.

In family KTCN-014, a maximum two-point parametric LOD score of 4.1 was obtained for the reduced penetrance analysis and a LOD score of 3.2 for the affected only analysis; both LOD scores occurred at marker D13S159 ($\theta = 0.0$). Table 1 displays parametric two-point LOD scores for the reduced penetrance model for all microsatellites within the linkage region on chromosome 13. Genotyping data from a 250 k Nsp array (Affymetrix) in family KTCN-014 revealed similar multipoint parametric LOD and NPL LOD scores. A maximum multipoint LOD score of 4.12 was observed at markers rs9561930~rs7339158, and rs774693~rs17473024 (Table 2) and reduced the genetic interval from a 12.0-Mb to a 5.59-Mb region between SNPs rs9516572 to rs3825523 on 13q32. Genotypes and haplotypes of 13q32 for family KTCN-014 are presented in Figure 2. The relationship of the pedigree members was confirmed by analyzing >5000 marker loci using the GRR program.³⁰ This program evaluates relationship of individuals by evaluating the proportion of alleles that are identical by state. We confirmed that the relationship of all pedigree members is consistent with the pedigree structure and that the four founders are unrelated to one other.

Figure 3 summarizes the full results of the genomewide scan for family KTCN-014 and shows a multipoint NPL LOD score of 3.2 obtained in this region. Haplotype analysis identified the risk haplotype shared by all affected individuals, one unaffected (KTCN 14-13) and one individual with unknown status (KTCN 14-21). Ocular examination performed for individual 14-13 at age 53 did not reveal KTCN. Since KTCN demonstrates reduced penetrance, we speculate that this individual with normal phenotype at age of 53 and an “at risk” haplotype is nonpenetrant for the KTCN phenotype. Individual 14-21 was 14 at the time of examination, presented with no KTCN and the “unknown” status was assigned in accordance with the criteria applied to all families. We speculate that this individual with normal phenotype and “at risk” genotype may develop KTCN when older.

Cytogenetic analysis and array CGH did not show any copy number variations on 13q32.

Discussion

We report a novel KTCN locus on 13q32. Several loci have been identified for KTCN. 11,13-18 A locus for autosomal dominant KTCN was mapped in Finnish families¹⁶ on 16q22.3-q23.1.¹⁶ Another locus on 15q22.33-24.2 was reported in a three-generation Northern Irish family whose affected individuals presented with combined early-onset autosomal dominant anterior polar cataract and KTCN and candidate genes *CTSH*, *CRABP1*, *IREB2*, and *RAS-GRF1* were excluded.¹¹ Other combined disease phenotypes were mapped to 17p13 in a two-generation Pakistani family with autosomal recessive Leber congenital amaurosis and KTCN.³¹ A locus on chromosome 3 was mapped to 3p14-q13 in a two-generational Italian family with autosomal dominant KTCN.¹⁴ Mutation analysis of *COL8A1*, the candidate gene located within the genetic region, did not show any pathogenic mutation.¹⁴ An additional locus for KTCN was identified using the genomewide scan approach on 5q14.3-q21.1 in a four-generation autosomal dominant white pedigree.¹⁵ A

locus on 2p24 was identified in a heterogeneous population of 28 families recruited in France, Spain, and Guadeloupe, of European, Arab, and Caribbean-African descent.¹³

Mutations in two genes have been evaluated as the cause of disease etiology. Mutations in the *VSX1* homeobox gene (locus on 20p11.21, KTCN1) were reported to cause posterior polymorphous dystrophy (PPD) and KTCN18 and recently, in another study, a heterozygous genomic 7-bp deletion in intron 2 of a *SOD1* gene was identified in two pedigrees with three affected patients with KTCN.¹⁹ Aldave et al.³² performed direct sequencing of the *VSX1* gene in 100 unrelated patients with KTCN; of the four mutations in the *VSX1* gene, only one was identified in a single affected patient. We detected no causative mutation in *VSX1*. In our study, several SNPs were identified, but those that were identified in affected individuals were also found in unaffected relatives and in normal ethnically matched individuals. These data suggest that the genetic cause(s) of KTCN in these families is (are) not due to mutations in the coding region of *VSX1*. It is possible that intronic mutations or mutations that affect the promoter region of *VSX1* could be present and not detected by our mutation analysis. For this reason, a linkage study with markers that map to chromosome 20 was performed and showed no evidence for linkage between KTCN and the microsatellite markers at that locus (data not shown). These findings exclude this locus as a candidate for KTCN in this population.

A similar approach was followed for *SOD1*, in which a heterozygous genomic 7-bp deletion in intron 2 was identified in three individuals with KTCN.¹⁹ No causative mutations were detected in *SOD1* in these Ecuadorian families. Genotyping with microsatellite markers from chromosome 21, region q22 excluded *SOD1* as a candidate for KTCN in this population.

Our results suggest that the KTCN gene in the cohort from Ecuador does not map to any previously described candidate locus. Only family KTCN-014 displayed linkage to 13q32. Although we tried to minimize the genetic heterogeneity by studying families from a single population, these results are not surprising, since KTCN is genetically heterogeneous with many previously reported loci.

Although no linkage studies have previously implicated this region in familial KTCN, it is interesting to note that a sporadic case of KTCN was observed to have a chromosomal abnormality involving a 13q ring abnormality designated as 46,XX,r(13)(p11q34).ish r(13)(p11q34)(85A10–).³³ The 19-year-old female patient had no atopy and no family history of ocular problems. The 13q32 region is a known locus for neocentromere formation,³⁴ resulting in chromosomal imbalances: Tetrasomy of 13q32-qter has been observed, with eye abnormalities including agenesia, microphthalmia, iris, and choroidal colobomata.³⁵ These findings could be consistent with the presence of a dosage-sensitive locus on 13q that causes ocular anomalies. Since array CGH is an effective tool for analyzing copy number variation,³⁶ this and other cytogenetic analyses were performed to verify this hypothesis in several individuals from family KTCN-014. Our analyses did not reveal any copy number variation on 13p32 in the tested individuals. However, although we applied an ultra-high-density array, it is possible that small deletion or duplications were missed.

The 5.6-Mb locus we identified on 13q32 contains 23 known transcripts (Ensembl).²⁹ Candidate genes include muscleblind-like protein 2 (*MBNL2* [MIM 607327]), *FERM*, *RhoGEF*, and pleckstrin domain-containing protein 1 (chondrocyte-derived ezrin-like protein; *FARP1* [MIM 602654]), ring finger protein 113B (*RNF113B*), dedicator of cytokinesis 9 (*DOCK9* [MIM 607325]), phosphoglycerate dehydrogenase like 1 (*PHGDHL1*), zinc finger protein of the cerebellum 5 (*ZIC5*), zinc finger protein of the cerebellum 2 (*ZIC2* [MIM 603073]), four repeat voltage-gated ion channel (*VGCNLI*), and fibroblast growth factor 14 (*FGF14* [MIM 601515]). These candidate genes are currently being screened for a possible role in the pathogenesis of KTCN.

In summary, the present study provides evidence of KTCN susceptibility loci on 13q32. Further studies are needed to delineate the role of other potential loci involved in KTCN in the families of different geographic origins.

Acknowledgments

The authors thank Kristen A. Bailey for assistance with data checking and pedigree analyses.

Supported by National Institutes of Health (NIH) Grant 1R01 EY015428.

References

1. Rabinowitz YS. Keratoconus Surv Ophthalmol. 1998; 42:297–319. [PubMed: 9493273]
2. Li X, Yang H, Rabinowitz YS. Longitudinal study of keratoconus progression. Exp Eye Res. 2007; 85:502–507. [PubMed: 17681291]
3. Cullen JF, Butler HG. Mongolism (Down's Syndrome) and keratoconus. Br J Ophthalmol. 1963; 47:321–330. [PubMed: 14189698]
4. Elder MJ. Leber congenital amaurosis and its association with keratoconus and keratoglobus. J Pediatr Ophthalmol Strabismus. 1994; 31:38–40. [PubMed: 8195961]
5. Beckh U, Schonherr U, Naumann GO. Autosomal dominant keratoconus as the chief ocular symptom in Lobstein osteogenesis imperfecta tarda (in German). Klinische Monatsblätter für Augenheilkunde. 1995; 206:268–272. [PubMed: 7791289]
6. Wajntal A, Koiffmann CP, Mendonca BB, et al. GAPO syndrome (McKusick 23074): a connective tissue disorder—report on two affected sibs and on the pathologic findings in the older. Am J Med Genet. 1990; 37:213–223. [PubMed: 2248288]
7. Kuming BS, Joffe L. Ehlers-Danlos syndrome associated with keratoconus: a case report. S Afr Med J. 1977; 52:403–405. [PubMed: 897848]
8. Robertson I. Keratoconus and the Ehlers-Danlos syndrome: a new aspect of keratoconus. Med J Aust. 1975; 1:571–573. [PubMed: 1143149]
9. Barr JT, Wilson BS, Gordon MO, et al. Estimation of the incidence and factors predictive of corneal scarring in the Collaborative Longitudinal Evaluation of Keratoconus (CLEK) Study. Cornea. 2006; 25:16–25. [PubMed: 16331035]
10. Jafri B, Lichter H, Stulting RD. Asymmetric keratoconus attributed to eye rubbing. Cornea. 2004; 23:560–564. [PubMed: 15256993]
11. Hughes AE, Dash DP, Jackson AJ, Frazer DG, Silvestri G. Familial keratoconus with cataract: linkage to the long arm of chromosome 15 and exclusion of candidate genes. Invest Ophthalmol Vis Sci. 2003; 44:5063–5066. [PubMed: 14638698]
12. Edwards M, McGhee CN, Dean S. The genetics of keratoconus. Clin Exp Ophthalmol. 2001; 29:345–351.
13. Hutchings H, Ginisty H, Le Gallo M, et al. Identification of a new locus for isolated familial keratoconus at 2p24. J Med Genet. 2005; 42:88–94. [PubMed: 15635082]

14. Brancati F, Valente EM, Sarkozy A, et al. A locus for autosomal dominant keratoconus maps to human chromosome 3p14-q13. *J Med Genet.* 2004; 41:188–192. [PubMed: 14985379]
15. Tang YG, Rabinowitz YS, Taylor KD, Li X, Hu M, Picornell Y, Yang H. Genomewide linkage scan in a multigeneration Caucasian pedigree identifies a novel locus for keratoconus on chromosome 5q14.3-q21.1. *Genet Med.* 2005; 7:397–405. [PubMed: 16024971]
16. Tyynismaa H, Sistonen P, Tuupanen S, et al. A locus for autosomal dominant keratoconus: linkage to 16q22.3-q23.1 in Finnish families. *Invest Ophthalmol Vis Sci.* 2002; 43:3160–3164. [PubMed: 12356819]
17. Fullerton J, Paprocki P, Foote S, Mackey DA, Williamson R, Forrest S. Identity-by-descent approach to gene localisation in eight individuals affected by keratoconus from north-west Tasmania, Australia. *Hum Genet.* 2002; 110:462–470. [PubMed: 12073017]
18. Heon E, Greenberg A, Kopp KK, et al. VSX1: a gene for posterior polymorphous dystrophy and keratoconus. *Hum Mol Genet.* 2002; 11:1029–1036. [PubMed: 11978762]
19. Udar N, Atilano SR, Brown DJ, et al. SOD1: a candidate gene for keratoconus. *Invest Ophthalmol Vis Sci.* 2006; 47:3345–3351. [PubMed: 16877401]
20. Matisse TC, Chen F, Chen W, et al. A second-generation combined linkage physical map of the human genome. *Genome Res.* 2007; 17:1783–1786. [PubMed: 17989245]
21. Shaffer LG, McCaskill C, Han JY, et al. Molecular characterization of de novo secondary trisomy 13. *Am J Hum Genet.* 1994; 55:968–974. [PubMed: 7977360]
22. O'Connell JR, Weeks DE. PedCheck: a program for identification of genotype incompatibilities in linkage analysis. *Am J Hum Genet.* 1998; 63:259–266. [PubMed: 9634505]
23. Abecasis GR, Cherny SS, Cookson WO, Cardon LR. Merlin-rapid analysis of dense genetic maps using sparse gene flow trees. *Nat Genet.* 2002; 30:97–101. [PubMed: 11731797]
24. Cottingham RW Jr, Idury RM, Schaffer AA. Faster sequential genetic linkage computations. *Am J Hum Genet.* 1993; 53:252–263. [PubMed: 8317490]
25. Ott, J. *Analysis of Human Genetic Linkage.* Baltimore: Johns Hopkins University Press; 1991.
26. Gudbjartsson DF, Jonasson K, Frigge ML, Kong A. Allegro, a new computer program for multipoint linkage analysis. *Nat Genet.* 2000; 25:12–13. [PubMed: 10802644]
27. Weeks DE, Sobel E, O'Connell JR, Lange K. Computer programs for multilocus haplotyping of general pedigrees. *Am J Hum Genet.* 1995; 56:1506–1507. [PubMed: 7762577]
28. Sobel E, Lange K. Descent graphs in pedigree analysis: applications to haplotyping, location scores, and marker-sharing statistics. *Am J Hum Genet.* 1996; 58:1323–1337. [PubMed: 8651310]
29. Hubbard TJP, Aken BL, Beal K, et al. Ensembl 2007. *Nucleic Acids Res.* 2007; 35:D610–D617. [PubMed: 17148474]
30. Abecasis GR, Cherny SS, Cookson WO, Cardon LR. GRR: graphical representation of relationship errors. *Bioinformatics.* 2001; 17(8):742–743. [PubMed: 11524377]
31. Hameed A, Khaliq S, Ismail M, et al. A novel locus for Leber congenital amaurosis (LCA4) with anterior keratoconus mapping to chromosome 17p13. *Invest Ophthalmol Vis Sci.* 2000; 41:629–633. [PubMed: 10711674]
32. Aldave AJ, Yellore VS, Salem, et al. No VSX1 gene mutations associated with keratoconus. *Invest Ophthalmol Vis Sci.* 2006; 47:2820–2822. [PubMed: 16799019]
33. Heaven CJ, Lalloo F, McHale E. Keratoconus associated with chromosome 13 ring abnormality. *Br J Ophthalmol.* 2000; 84:1079. [PubMed: 11032444]
34. Alonso A, Mahmood R, Li S, Cheung F, Yoda K, Warburton PE. Genomic microarray analysis reveals distinct locations for the CENP-A binding domains in three human chromosome 13q32 neocentromeres. *Hum Mol Genet.* 2003; 12:2711–2721. [PubMed: 12928482]
35. Warburton PE, Dolled M, Mahmood R, et al. Molecular cytogenetic analysis of eight inversion duplications of human chromosome 13q that each contain a neocentromere. *Am J Hum Genet.* 2000; 66:1794–1806. [PubMed: 10777715]
36. Carter NP. Methods and strategies for analyzing copy number variation using DNA microarrays. *Nat Genet.* 2007; 39:S16–21. [PubMed: 17597776]

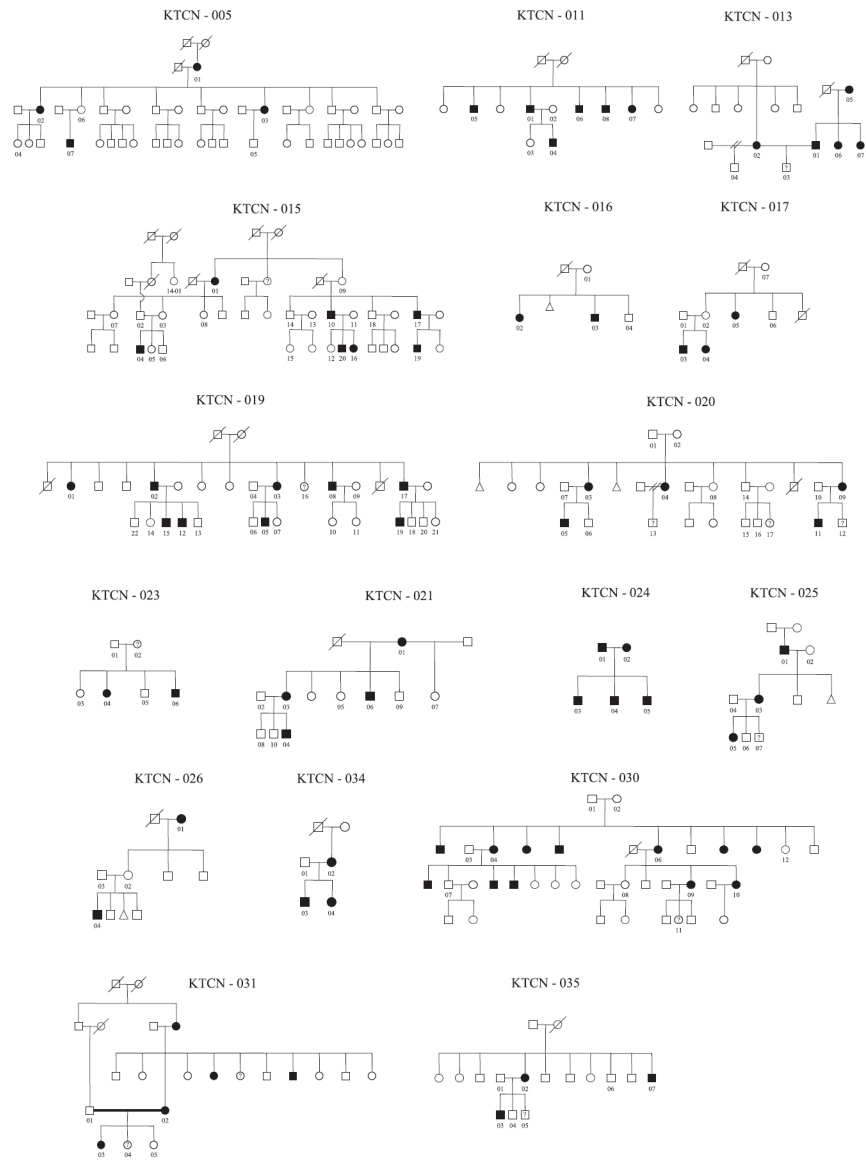


Figure 1. Pedigrees of the 17 of 18 Ecuadorian families with familial KTCN. *Filled symbols:* individuals with KTCN; *open symbols:* unaffected individuals; *symbols with question mark:* individuals with unknown disease status.

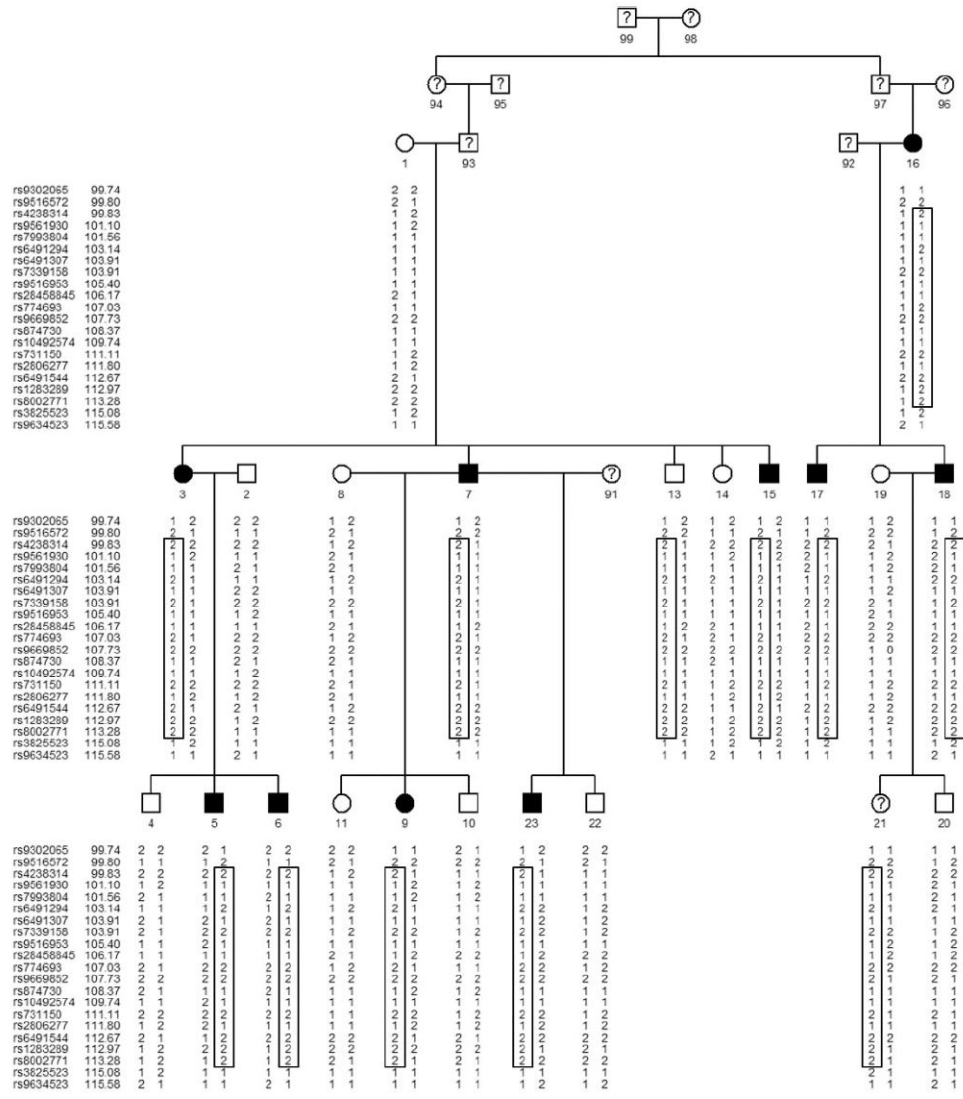


Figure 2. Pedigree of family KTCN-014. *Filled symbols:* individuals with KTCN; *open symbols:* individuals who have undergone examination and have no KTCN; *symbols with question mark:* individuals with unknown KTCN status. Below each individual is shown the haplotypes for the 13q32 chromosomal region. Because of the large number of SNPs within the region, only one SNP approximately every 250 kb, with a minor allele frequency of >0.2 is shown. The haplotype that segregates with KTCN is highlighted in gray and is flanked proximally by marker rs9516572 (94,801,664 bp) and distally by marker rs3825523 (100,391,121 bp).

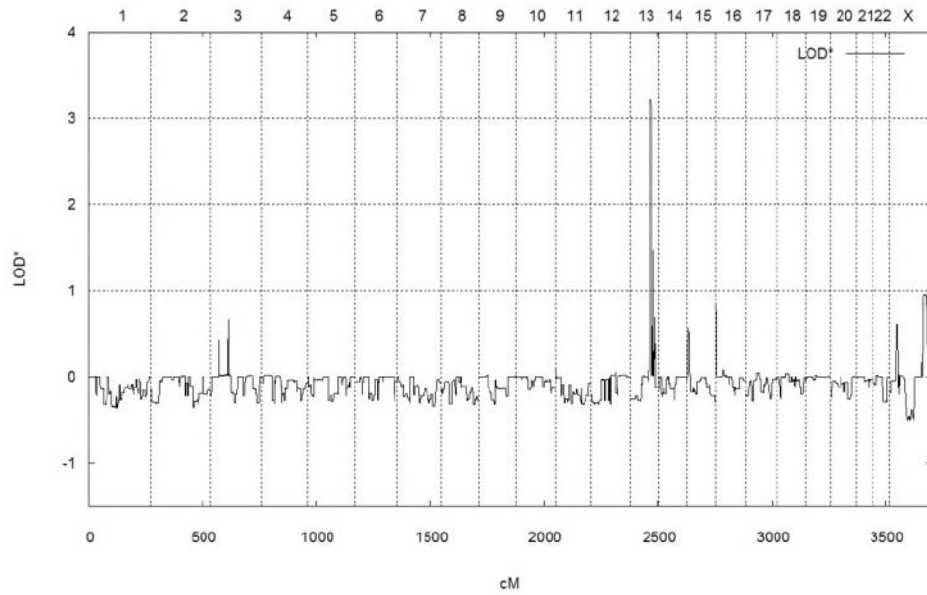


Figure 3. Results of the multipoint nonparametric linkage analysis for family KTCN-14. The x -axis represents the chromosomal location for each of the 22 autosomes, and the y -axis represents the NPL-LOD using the “All” Kong-Cox exponential model. The highest peak is on 13q32.1-q32.3 with a maximum NPL-LOD of 3.2.

Table 1

Two-Point Parametric Linkage Analysis Results of STR Marker Loci on Chromosome 13q in Family KTCN-014

Marker Names	Physical position (bp) [*]	Genetic position (cM) [†]	Two-Point LOD θ (All/Affected Only)											
			0.00	0.01	0.05	0.10	0.20	0.30						
D13S1306 [‡]	76,543,318	72.45	-8.15/-6.05	-5.62/-4.12	-2.92/-2.84	-1.62/-2.09	-0.50/-1.06	-0.05/-0.48						
D13S170	80,007,094	75.63	-6.66/-5.99	-2.12/-2.89	-0.29/-1.07	0.35/-0.39	0.70/0.09	0.64/0.20						
D13S265[§]	89,170,920	80.90	-5.88/-4.85	-2.44/-2.84	-0.60/-1.13	0.06/-0.45	0.47/0.05	0.48/0.17						
D13S1241	96,348,300	88.93	3.09/2.11	3.04/2.07	2.82/1.89	2.52/1.66	1.91/1.22	1.26/0.80						
D13S1823	96,616,816	89.31	1.23/1.34	1.20/1.31	1.09/1.17	0.95/1.01	0.69/0.69	0.44/0.41						
D13S793	96,749,903	89.31	1.29/1.01	1.28/1.00	1.23/0.95	1.15/0.88	0.95/0.70	0.69/0.49						
D13S1252	97,335,372	90.21	2.91/1.66	2.86/1.62	2.63/1.48	2.34/1.30	1.75/0.96	1.17/0.63						
D13S1298	97,823,725	91.53	2.13/2.03	2.09/1.99	1.93/1.81	1.72/1.59	1.28/1.14	0.84/0.70						
D13S159	97,851,594	91.53	4.05/3.16	3.98/3.11	3.72/2.88	3.37/2.58	2.62/1.97	1.81/1.32						
D13S770	98,429,336	92.10	3.61/2.56	3.55/2.51	3.30/2.31	2.98/2.04	2.28/1.50	1.54/0.97						
D13S1284	98,687,256	93.00	2.66/1.70	2.61/1.66	2.42/1.51	2.17/1.31	1.63/0.92	1.07/0.56						
D13S1232	99,268,672	93.29	3.46/2.84	3.40/2.79	3.16/2.57	2.84/2.29	2.16/1.71	1.45/1.12						
D13S1267	99,695,125	94.36	1.87/1.20	1.84/1.17	1.71/1.05	1.54/0.91	1.17/0.63	0.78/0.38						
D13S1240	99,966,808	94.69	2.52/2.00	2.48/1.96	2.30/1.78	2.07/1.55	1.56/1.10	1.03/0.67						
D13S779	100,301,956	95.40	1.71/1.17	1.67/1.15	1.53/1.07	1.35/0.96	1.02/0.73	0.70/0.49						
D13S225	100,344,377	96.46	2.76/1.65	2.71/1.61	2.51/1.45	2.25/1.25	1.70/0.86	1.11/0.50						
D13S1323	101,318,181	97.85	-0.47/-0.57	0.06/-0.03	0.51/0.43	0.62/0.54	0.52/0.48	0.29/0.32						
D13S1256	102,098,641	98.48	3.57/2.38	3.51/2.33	3.27/2.13	2.94/1.88	2.25/1.37	1.51/0.87						
D13S274	103,359,144	100.31	0.73/-0.61	1.32/-0.05	1.75/0.43	1.79/0.57	1.53/0.55	1.09/0.41						
D13S286	105,735,686	107.20	1.63/1.65	1.61/1.62	1.51/1.49	1.38/1.32	1.09/0.99	0.77/0.67						
D13S173	106,604,889	108.87	2.60/1.98	2.56/1.94	2.41/1.78	2.19/1.57	1.71/1.15	1.17/0.75						
D13S1265	108,126,457	113.04	-3.58/-3.00	-1.34/-1.32	-0.12/-0.19	0.34/0.23	0.63/0.48	0.59/0.46						
D13S285	111,843,382	123.98	-3.68/-2.70	-1.92/-1.03	-0.55/0.06	0.05/0.45	0.47/0.62	0.50/0.52						

For each theta value, the two-point parametric LOD score is given for the reduced penetrance analysis followed by the affected-only analysis (after the shift). STR, short tandem repeat.

^{*} NCBI[build] 36.1 genome assembly.[†] The Rutgers Combined Linkage-Physical Map of The Human Genome (Build 36).

¶ Whole genome scan markers are displayed in italics.

§ Markers displayed in bold flank the haplotype.

Author Manuscript

Author Manuscript

Author Manuscript

Author Manuscript

Multipoint Linkage Analysis Results, for Reduced Penetrance Analysis, Affected-Only Analysis, and Nonparametric Analysis, for SNP Marker Loci on 13q Selected Every 250 k with Minor Allele Frequency >0.2 in Family KTCN-014

Table 2

Marker Names		Physical Position (bp)*	Genetic Position (cM) [†]	Mpt LOD		
Affymetrix ID	NCBI ID			Parametric	Aff Only	NPL
SNP A-2036775	rs9589816	93,183,430	95.03000	-2.713	-2.7517	0.0651
				-1.238	-1.2980	0.0912
SNP A-2129772	rs1888229	93,386,359	95.31095	-0.943	-1.0004	0.1184
				-0.558	-0.6328	0.1900
SNP A-1824693	rs835981	93,588,673	96.02410	-0.374	-0.4382	0.2569
				-0.070	-0.1575	0.3786
SNP A-2175043	rs9524473	93,838,819	96.44000	0.002	0.0077	0.4785
				0.033	0.0010	0.4803
SNP A-4229612	rs1112370	94,044,441	97.05000	0.012	-0.0142	0.4816
				0.041	0.0083	0.4846
SNP A-2156320	rs9561694	94,251,072	98.07000	0.018	0.0223	0.4871
				0.044	0.0269	0.4881
SNP A-1873635	rs766606	94,452,168	98.54000	0.020	0.0241	0.4887
				0.045	0.0131	0.4883
SNP A-4204335	rs4773844	94,653,501	98.54000	0.020	-0.0060	0.4875
				0.029	-0.0044	0.4877
SNP A-2233637	rs9302065	94,769,017	99.74205	0.021	-0.0055	0.4879
				0.021	-0.0053	0.4879
SNP A-2175799	rs9516572	94,801,664	99.80156	0.562	-0.0054	0.4879
				2.620	1.8644	1.7755
SNP A-4202625	rs4238314	94,816,547	99.82870	2.922	2.1625	2.0756
				3.326	2.5339	2.4482
SNP A-4194428	rs2993570	94,857,025	100.09892	3.533	2.7311	2.6458
				3.924	3.0988	3.0138
SNP A-2023389	rs9561930	95,140,023	101.10133	4.127	3.2951	3.2102
				4.127	3.2951	3.2102

Marker Names		Mpt LOD				
Affymetrix ID	NCBI ID	Physical Position (bp)*	Genetic Position (cM) [†]	Parametric	Aff Only	NPL
SNP A-1925413	rs1980942	95,374,525	101.56000	4.127	3.2951	3.2102
SNP A-2176177	rs7993804	95,610,858	101.56000	4.127	3.2952	3.2102
SNP A-4229714	rs912690	95,818,706	103.14000	4.127	3.2953	3.2103
SNP A-2028215	rs6491294	95,925,710	103.14000	4.127	3.2953	3.2103
SNP A-4231882	rs506757	96,101,710	103.14000	4.127	3.2953	3.2103
SNP A-4229741	rs6491307	96,252,811	103.91000	4.127	3.2953	3.2102
SNP A-2045804	rs11069247	96,313,752	103.91000	4.127	3.2953	3.2102
SNP A-2176714	rs4771979	96,533,786	103.91000	4.127	3.2952	3.2102
SNP A-2123283	rs7339158	96,631,324	103.91000	4.127	3.2952	3.2102
SNP A-4187294	rs4441122	96,751,047	104.61199	3.923	3.2950	3.2100
SNP A-1837153	rs9516953	96,970,509	105.40036	3.525	3.2949	3.2099
SNP A-1818113	rs2793698	97,187,358	105.75410	3.525	3.2948	3.2098
SNP A-2131530	rs28458845	97,283,653	106.16804	3.525	3.2948	3.2098
SNP A-4229787	rs624066	97,443,856	106.99800	3.809	3.2949	3.2099
SNP A-2177343	rs774693	97,597,584	107.03000	3.929	3.2949	3.2099
				4.039	3.2949	3.2099
				4.127	3.2950	3.2100
				4.127	3.2950	3.2099

Marker Names				Mpt LOD		
Affymetrix ID	NCBI ID	Physical Position (bp)*	Genetic Position (cM) [†]	Parametric	Aff Only	NPL
SNP A-4236367	rs7325009	97,679,564	107.28920	4.126	3.2949	3.2099
SNP A-2270431	rs9669852	97,883,413	107.73000	4.126	3.2948	3.2098
SNP A-2089049	rs3752973	97,895,510	107.73000	4.125	3.2947	3.2097
SNP A-4225877	rs2211647	98,101,412	107.77392	4.125	3.2947	3.2097
SNP A-2232456	rs874730	98,220,386	108.37345	4.125	3.2945	3.2095
SNP A-2122159	rs7320305	98,342,974	109.07106	4.125	3.2944	3.2094
SNP A-2177988	rs10492574	98,494,931	109.74083	4.125	3.2943	3.2093
SNP A-1867598	rs7989020	98,600,789	110.20741	4.124	3.2942	3.2092
SNP A-2310974	rs731150	98,805,551	111.10992	4.124	3.2941	3.2091
SNP A-2243897	rs17473024	99,036,194	111.80000	4.124	3.2940	3.2090
SNP A-1939047	rs2806277	99,176,470	111.80000	4.124	3.2938	3.2088
SNP A-4229904	rs2761171	99,278,898	111.80000	4.123	3.2936	3.2086
SNP A-2178627	rs6491544	99,549,209	112.67000	4.122	3.2934	3.2084
SNP A-2149444	rs9557412	99,749,857	112.67000	4.121	3.2932	3.2082
SNP A-2003518	rs1283289	99,915,625	112.97451	4.120	3.2928	3.2078
				4.119	3.2924	3.2074
				4.118	3.2917	3.2067
				4.119	3.2910	3.2060
				4.119	3.2902	3.2052
				4.119	3.2895	3.2044
				4.118	3.2887	3.2037
				4.118	3.2879	3.2029
				4.113	3.2839	3.1988
				4.109	3.2799	3.1949
				4.103	3.2750	3.1899
				4.098	3.2701	3.1850
				4.085	3.2608	3.1758
				4.072	3.2514	3.1664
				4.067	3.2468	3.1617

Marker Names			Mpt LOD			
Affymetrix ID	NCBI ID	Physical Position (bp)*	Genetic Position (cM) [†]	Parametric	Aff Only	NPL
SNP A-2064788	rs837290	99,954,494	113.01420	4.061	3.2420	3.1570
SNP A-1846263	rs1283206	100,164,852	113.22898	4.034	3.2172	3.1321
SNP A-2051423	rs8002771	<i>100,233,149</i>	<i>113.28000</i>	3.969	<i>3.1539</i>	<i>3.0687</i>
SNP A-2119104	rs4238226	100,372,469	113.96084	3.744	2.9303	2.8447
SNP_A-2276131	rs3825523	100,391,121	115.07971	1.127	0.2924	0.0171
SNP A-1935501	rs9634523	<i>100,401,546</i>	<i>115.58000</i>	1.127	<i>0.3145</i>	<i>0.0177</i>
SNP A-2202696	rs4772360	100,576,615	115.86901	1.428	0.4932	0.0404
SNP A-2296459	rs3858788	100,799,522	116.70346	1.542	0.5435	0.1285
SNP A-2132148	rs972366	101,004,875	117.47220	1.603	0.5795	0.2037
SNP A-1873094	rs1927712	101,209,047	118.07735	1.671	0.5796	0.2076
SNP A-1783335	rs1581743	101,437,372	118.36759	1.728	0.5726	0.1980
SNP A-4220324	rs1336706	101,646,552	118.51837	1.728	0.5370	0.1330
SNP A-2282551	rs9518729	101,901,616	118.70223	1.728	0.4908	0.0523
				1.515	0.3925	0.0212
				1.077	0.2525	0.0154
				2.059	1.1920	1.0604
				2.340	1.4487	1.3416
				2.478	1.5775	1.4789
				2.575	1.6609	1.5667

Markers in italics are also displayed in Figure 2. Markers shown in bold flank the haplotype.

* NCBI build 36.1 genome assembly.

[†] Genetic positions of SNP marker loci were interpolated using the Rutgers' Combined Physical and Genetic map of the Human genome.